CHAIR ENERGY & PROSPERITY
Energy Transition Pathways and Financing

Working Paper

A simple phenomenological model of the world population dynamics

Victor Court and Florent Mc Isaac*

November 19, 2018

Contact: Victor Court, v.court@sussex.ac.uk

* Victor Court (email: v.court@sussex.ac.uk): Science Policy Research Unit (SPRU), Business School, University of Sussex, Jubilee, Brighton BN1 9SL, UK; and Chair Energy & Prosperity, Institut Louis Bachelier, 28 place de la Bourse, 75002 Paris, France. Florent Mc Isaac (email: mcisaacf@afd.fr): Agence Française de Développement, 5 rue Roland Barthes, 75012 Paris, France; and Chair Energy & Prosperity, Institut Louis Bachelier, 28 place de la Bourse, 75002 Paris, France.

La Chaire Energie et Prospérité

La chaire Energie et Prospérité a été créée en 2015 pour éclairer les décisions des acteurs publics et privés dans le pilotage de la transition énergétique. Les travaux de recherche conduits s'attachent aux impacts de la transition énergétique sur les économies (croissance, emploi, dette), sur les secteurs d'activité (transport, construction, production d'énergie, finance) et aux modes de financement associés. Hébergée par la Fondation du Risque, la chaire bénéficie du soutien de l'ADEME, d'Air Liquide, de l'Agence Française de Développement, de la Caisse des Dépôts, de Mirova, de Schneider Electric et de la SNCF.

Les opinions exprimées dans ce papier sont celles de son (ses) auteur(s) et ne reflètent pas nécessairement celles de la Chaire Energie et Prospérité. Ce document est publié sous l'entière responsabilité de son (ses) auteur(s).

Les Working Papers de la Chaire Energie et Prospérité sont téléchargeables ici :

http://www.chair-energy-prosperity.org/category/publications/

Chair Energy and Prosperity

The Energy and Prosperity academic Chair was created in 2015 to inform decisions of public and private actors in managing the energy transition. The Chair research deals with the impacts of energy transition on national economies (growth, employment, debt), on specific sectors (transportation, construction, energy, finance) and with the associated financing issues. Hosted by the Risk Foundation, the chair has the support of ADEME, Air Liquide, the French Development Agency, the Caisse des Dépôts, Mirova, Schneider Electric, and SNCF.

The opinions expressed in this paper are those of the author(s) and do not necessarily reflect the position of Chair Energy and Prosperity. It is therefore published under the sole responsibility of its author(s).

Working Papers from the Chair Energy and Prosperity can be downloaded here:
http://www.chair-energy-prosperity.org/en/category/publications-2/

A Simple Phenomenological Model of the World Population Dynamics

Victor Court and Florent Mc Isaac*

November 19, 2018

Abstract

In this article, we design a phenomenological model of the global human population dynamics by using the gross world product (GWP) as an exogenous input variable to determine the birth rate and death rates of each age group. Using a historical fit, we show that our model accurately reproduces the global population dynamics over the period 1950–2015. Under prospective GWP scenarios, our model yields very similar outputs for any increasing GWP trajectory. A major implication of this simulation result is that both the United Nations and the IPCC take no account of the historical relationship that prevailed between GWP and population from 1950 to 2015, and thus assume future decoupling possibilities between economic development and fertility that have never been witnessed during the last sixty-five years. Moreover, in the case of an abrupt collapse of the economic production, the population dynamics of our model responds with higher deaths rates that are more than offset by increasing birth rates, leading to a relatively larger and younger population. Finally, as the main purpose of our analytical framework is incorporation into Integrated Assessment Models, we investigate the response of our model to an excess mortality function associated with climate change. Estimates of additional deaths per five-year period due to climate change in 2100 range from 1 million in a +2°C scenario to 6 million in a +4°C scenario.

Keywords: Demographic transition; Global population model; System dynamics; Climate change.

JEL Classification: J11, J21, C62, Q54.

*Victor Court (email: v.court@sussex.ac.uk): Science Policy Research Unit (SPRU), Business School, University of Sussex, Jubilee, Brighton BN1 9SL, UK; and Chair Energy & Prosperity, Institut Louis Bachelier, 28 place de la Bourse, 75002 Paris, France. Florent Mc Isaac (email: mcisaacf@afd.fr): Agence Française de Développement, 5 rue Roland Barthes, 75012 Paris, France; and Chair Energy & Prosperity, Institut Louis Bachelier, 28 place de la Bourse, 75002 Paris, France.

1 Introduction

Fossil energies, as a fundamental driver of the Industrial Revolution, started the era of anthropogenic climate change. The 2015 Paris Agreement attempts to combat Climate Change by establishing to goal of maintaining global temperatures to below $+2°$C temperature change compared to the pre-industrial era, among others goals, to avoid possible irreversible tipping points (IPCC, 2013). A worldwide agenda is now set in motion to design low-carbon economies. To face such a challenge, research teams around the globe have built numerous Integrated Assessment Models (IAMs) to help anticipating the economic challenges of meeting this target. In particular, IAMs are used to analyze climate change mitigation scenarios performed by the Working Group III (WGIII) of the Intergovernmental Panel on Climate Change (IPCC, 2014). Comparing 1,184 scenarios within 31 different IAMs,[1] surprisingly showed no endogenous feedback loop between anthropogenic climate change and population. We argue that the reason for this methodological choice is the absence of endogenous population dynamics (and sometimes technological change) in most IAMs. In Section 1.1 we review the evidence of past concerns on overpopulation that proved to be erroneous to show the complexity of human population dynamics. Then, in Section 1.2, we look at the current state of the literature on world population models in order to understand why these models are rarely used in larger economic models such as IAMs.

1.1 Overpopulation: old concerns die hard

Until approximately 300 years ago, world population growth has been very low, at around 0.04% per year, from four million people in 10,000 BCE to 610 millions in 1700. However, the Industrial Revolution drastically changed this pattern of long-lasting limited growth, and global population reached 1.2 billion individuals by 1850, which corresponds to an annual increase of 0.45% during the period 1700–1850 (Kremer, 1993). Several classical economists of the time raised concerns about such rapid population growth. By considering geometrical growth for the population dynamics, while food production followed an arithmetical increase due to decreasing returns on land, Malthus (1798) predicted that the English population would ultimately lack food supply, which could only result in unavoidable deaths by hunger and disease.[2] This prediction proved to be erroneous because Malthus did not reckon the massive yields increases that took place in the agricultural sector at the time (Smil, 2017, p. 114) .

As shown in Figure 1, from 1850 to 1920, the growth rate of the world population has slightly increased by about 0.55–0.60% per year, resulting in a global population of 1.8 billion. After 1920, another order of magnitude change can be observed. Exceeding 1% in the 1940s, the annual growth rate of the wold population steadily increased and reached its peak at 2.2% in 1962–63 with a global population of 3.15 billion (Kremer, 1993; United Nations, 2017b). At this point, the fear of overpopulation came back in several scholars' writing and, exactly 170 years after Malthus, Ehrlich became famous for his (pessimistic) predictions in *The Population Bomb* (1968). Again, those forecasts of impending world famines proved inaccurate due to an increase in food production from the conversion of forests to agricultural lands (Goldewijk et al., 2017) and agricultural yield improvements (Smil, 2017, p. 312).

[1] See Table A.II.14 in Annex II of IPCC (2014, pp. 1309–1310) for a summary of the 31 IAMs used in the Fifth Assessment Report of the WGIII.

[2] This initial formulation made Malthus both famous and infamous, but in later life he took a much more nuanced attitude to the balance between production and population. In particular, Malthus came to appreciate that nuptiality played a very important role in determining population trends, influencing both fertility levels, and indirectly, also mortality levels (Wrigley, 2016, pp. 24–25).

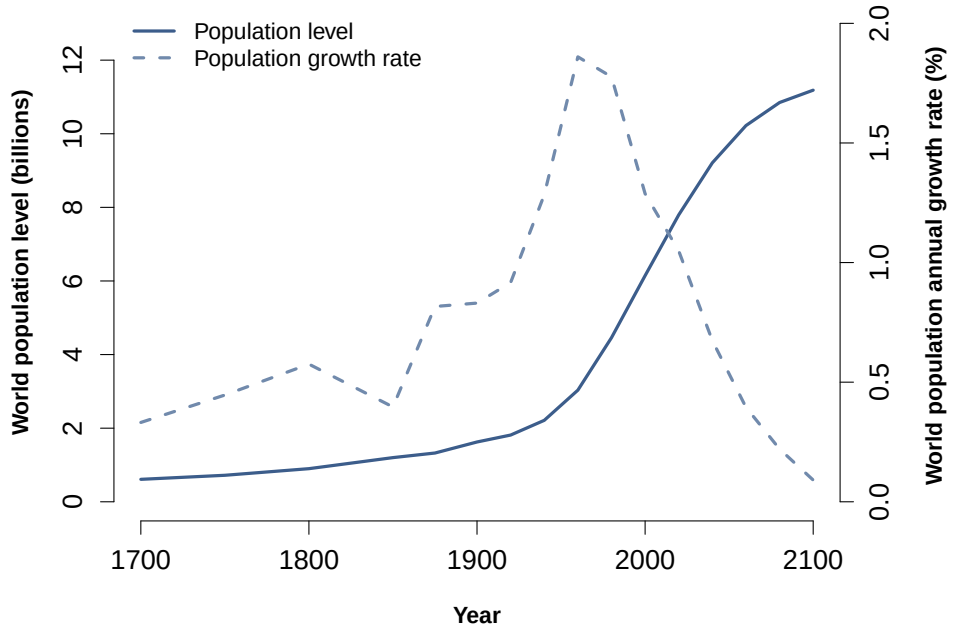

Figure 1: Historical and projected world population level (left axis) and annual growth rate (right axis), 1700–2100. Data source: Kremer (1993) from 1700 to 1950, United Nations's (2017b) medium estimate from 1950 to 2100.

As of 2015, the world population was about 7.4 billion and its annual growth rate was approximately 1.15%. Considering the United Nations's (2017b) medium projection of a growth rate reaching 0.09% per year at the end of this century, the global population would be just below 11.2 billion in 2100 (Figure 1). Accordingly, in November 2017, the concern about overpopulation was renewed in a statement of 15 364 scientists from 184 countries who indicated that humanity is jeopardizing its future by not reining in its "intense but geographically and demographically uneven material consumption and by not perceiving continued rapid population growth as a primary driver behind many ecological and even societal threats" (Ripple et al., 2017, p. 1026). The strong warning of Ripple et al. (2017) ends with thirteen proposed steps that mankind should undertake to transition towards a more environmentally sustainable alternative to the so-called business as usual. Among them, Ripple et al. (2017, p. 1028) suggest "estimating a scientifically defensible, sustainable human population size for the long term while rallying nations and leaders to support that vital goal".

Of course, for a given level of pollution, it is not the population level *per se* that represents a problem, but rather a combination of population with the level of per capita consumption, and the technological level defining the pollution by unit of consumption.[3] Since technological progress is not more foreseeable than before, one could argue that, once again, future innovations are going to alleviate the human population burden on Earth in the coming decades. For technological optimists, the current overpopulation concern will add to the list of failed overpopulation predictions of the past. However, no one can deny that food supply is heavily supported by the use of fossil fuels, either directly through fertilizers and mechanization, but also indirectly through the general use of

[3]This controversy is well illustrated by the $I = PAT$ equation, where I is the impact of human activity on the environment (i.e., the pollution level), P is the population level, A stands for affluence (i.e., the level of per capita consumption), and T represents the technological level. See Chertow (2000) for an historical analysis of the various forms the *IPAT* equation has taken since its formulation in the 1970s.

transport, industry, and services (Smil, 2017, pp. 306–313).

1.2 Literature review of human population models

When performing a review of the literature on global human population models, we identified three different classes of analytical frameworks that we labeled '*carrying capacity type models*', '*complex World3 type models*', and '*Cohort-component UN type models*' (Table 1).

The term *carrying capacity* is generally used in the literature to frame a stationary world population size that would ensure the stable coexistence of the biosphere and civilization in the long term. Since von Foerster et al. (1960), several articles have developed simple models where, omitting any consideration of age or sex structures, the world population is represented by a single variable that follows a (set of) differential equation(s).[4] The dynamics of such models depend on the exogenous definition of several parameters, with Earth's carrying capacity being the most crucial parameter. Accordingly, all these analytical frameworks belong to a first class of models analyzed in this section and hereafter labeled '*carrying capacity type models*'. The review of carrying capacity estimates performed by Cohen (1995) shows that (up to 1995) the 65 lower (respectively upper) bounds on human population was 7.7 (respec. 12) billion, with extreme estimates ranging from 1 to 1000 billion. In addition to the difficulty of estimating the carrying capacity parameter, which should furthermore evolve with environmental change, some of those models, such as Dolgonosov (2016) and Okuducu and Aral (2017), introduce another endogenous variable representing the informational, or knowledge, state of humanity. The general knowledge-related measure of civilization's progress, and the additional parameters that come with its formulation, hardly find a correspondence with real world data, which may cast further doubts on the calibration and prospective results of those models.[5] Alternatively, in a method closer to standard economic theory, Cai (2012), Guerrini (2013), and others introduce capital accumulation and production decisions to capture humanity's development level rather than a knowledge-related variable. Nevertheless, it is clear that the different *carrying capacity type models* can hardly be introduced into IAMs, because their representation of the global human population is too simple (no age structure), and abstract (relying on the carrying capacity of the Earth and other endogenous parameters).

A second class of models, hereafter labeled '*complex World3 type models*', corresponds to more complex analytical frameworks based on system dynamics. Such models explicitly feature an age structure by defining births and death rates that are specific to each age group. As a result, such models do not require the uncertain estimation of a parameter representing the carrying capacity of the Earth. Because of their higher degree of realism, models of this second group seem more meaningful for IAMs, yet they have not been widely implemented. This is because these models derive from the *World3* model of Meadows et al. (1972), and as this original source, one of their drawbacks is their lack of clarity and transparency. In particular, it is difficult to understand what exactly drives the dynamics of such kind of models. In recent versions, articles that adopt such frameworks either summarize a partial set of equations with a graphical representation (Cole and Flenley, 2008; Eberlein and Thompson, 2013; Navarro et al., 2017); or, on the contrary, suffer from high dimensionality and complexity (Micó et al., 2008, 2006; Sanz et al., 2014).

Finally, a third class of global population models, hereafter labeled '*cohort-component UN type models*', uses the United Nations's (2017a) accounting framework for fertility, mortality, and migrations. In such models, population is divided between males and females and five-year age groups. Such a precision comes at the expense of the need for three exogenous age-specific time series, namely sex ratios, death rates, and fertility rates.

[4] Akaev and Sadovnichii (2010) is a good introduction to this class of models.

[5] Aral (2014) has introduced climate change into an information-based model of this kind.

Table 1: Advantages and flaws of different world human population models.

	Advantages	Flaws
Carrying capacity type models	Tractable problem with closed-form solutions	Need to define the carrying capacity of the Earth
Complex World3 type models	Realist 5-years age structure	Opacity regarding driving mechanisms
Cohort-component UN type models	Realist sex and 5-years age structure	Need for three age-specific exogenous time series
Present article	Realist 5-years age structure, GWP is the only exogenous driver, model remains comprehensible	Possible difficulty to obtain closed-form solutions

1.3 Goal and organization of the paper

We argue that there is a lack of intermediate-size human population models that would both avoid the flaws and combine the advantages that respectively affect the three classes of models described *supra* and in Table 1. If possible, such an intermediate model should offer closed-form solutions without requiring the estimation of abstract parameters, in particular the carrying capacity of the Earth. In the meantime, such a model should be complex enough to feature an age structure without presenting the flaws of a highly dimensional black box.

A world population model, as the one developed in this paper, would be particularly appealing for IAMs. To the best of our knowledge, as of today IAMs mainly assume an exogenous population based on the UN cohort-component method and, therefore, take little, if any, consideration of potential feedback between climate change and population dynamics. Hence, in addition to the fact that the endogenous population model presented thereafter could be easily added to any IAM, it would also help to understand: (i) how climate change is likely to affect the population dynamics (through changes in the death rate(s), for instance); and (ii) how macroeconomics is impacted by such feedback, both in terms of available workforce and aggregate demand.

To design the world population model, we first present empirical facts regarding the birth rate and age-specific death rates in relation to gross world product (GWP) in Section 2. Those relations justify the set of equations defining our model of the world human population. Simulations of the model are performed in Section 3 in order to (i) compare its outputs with the historical estimates of the United Nations, and (ii) assess its sensitivity through four prospective scenarios. In Section 4, we discuss the need for changes to the model under a drastic regime change such as an economic collapse or due to climate change. Finally, a summary of the contributions to this article is given in Section 5, along with recommendations for future research.

2 Methods: from dataset to model

Prior to introducing the dataset, let us first sketch the methodology that will motivate the choices made throughout this section. The global population, N, is divided into n age groups, N_i, so that

$$N = \sum_{i=1}^{n} N_i.$$

The dynamics of each group i follows the law of motion,

$$\dot{N}_i = I_i - O_i, \qquad \forall i \in \{1, \ldots, n\} \tag{1}$$

where, I_i, is the inflow of population within the age group i (births or changes in age group), and, O_i, is the outflow of population within the age group i (deaths or changes age group). This section focuses on identifying the quantities (I_i, O_i) for each age group.

2.1 Ensuring the stock-flow consistency of the dataset

Figure 2 plots the stock of population from 1950 to 2015 for 14 age groups $(N_1, \ldots, N_{14})$ at a five-year frequency retrieved from the United Nations (2017b).[6] The ith group, N_i, for $i \in \{1, \ldots, 13\}$, represents the $[5(i-1), 4+5(i-1)]$ years-old age group. The last group, N_{14}, represents the population over 65 years-old. As a result of data granularity, the unit time between two periods (t and $t+1$) corresponds to 5, which is the number of years during which individuals remain in a given age-group.

When using the data for economic modeling purposes, a minimum of four distinct cohorts $(C_1, \ldots, C_4)$ can be identified out of the 14 age groups:

- $C_1 := \sum_{i=1}^{3} N_i$, the young inactive population from age 0 to 14;
- $C_2 := \sum_{i=4}^{10} N_i$, the young active population in childbearing age from 15 to 49;[7]
- $C_3 := \sum_{i=11}^{13} N_i$, the old active population from 50 to 64; and
- $C_4 := N_{14}$, the retired population away from the job market from 65 and over.[8]

Therefore, $C_2 + C_3$ represents the active population and would define the denominator of the employment rate in a broader economic model. The choice of 14 different age groups is motivated by the fact that transfer of population between one (economically meaningful) cohort to another strongly depends on the population structure itself. Indeed, if one assumes a constant (average) share of population transfer between cohorts (as in '*World-3* type models'), then a rather strong bias would appear in situation like the baby boom at the aftermath of WWII. The consequences of a misrepresentation of the first three cohorts can lead to misleading measurements of the (past and future) workforce and population inflow. However, we chose a simpler aggregated characterization for the last cohort dynamics as it is not the primary focus of our paper. Moreover, throughout our model we assume (i) a strict gender parity in population, and (ii) a uniform age distribution within each of the fourteen 5-year age groups.

[6] More precisely, two time series are used in this section: (i) File POP/7-1: Total population (both sexes combined) by five-year age group, region, sub-region and country, 1950–2100 (thousands); and (ii) File MORT/4-1: Deaths (both sexes combined) by five-year age group, region, sub-region and country, 1950–2100 (thousands).

[7] As a consequence of this modeling choice, we ignore the fact that some individuals, especially men, can have children after 49.

[8] Of course, in many countries there are now indications to push the retirement age further than 65. But here we are constrained by the United Nations data, which only has one age group above 65.

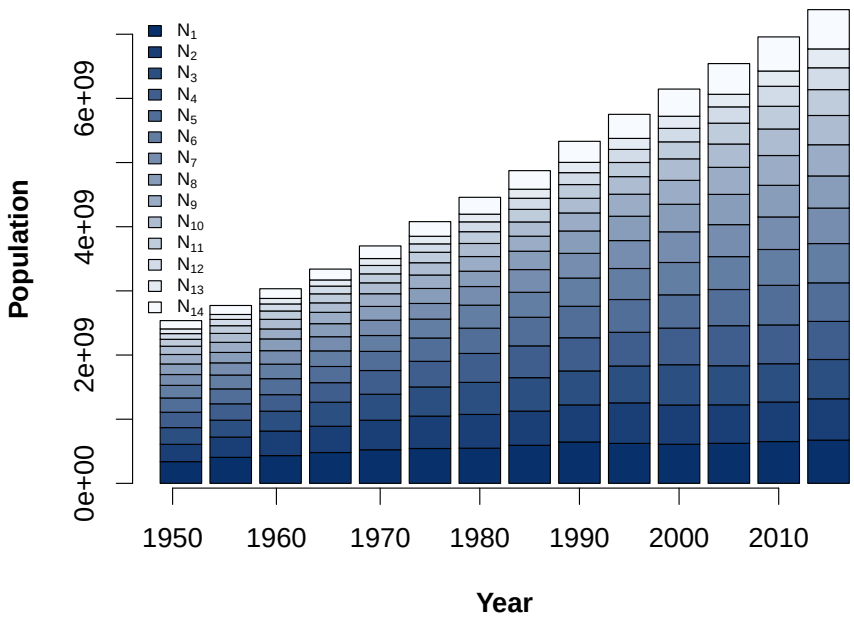

Figure 2: World population structure by five-year age groups, 1950–2015.

To ensure the stock-flow consistency of the data, we first define the global inflow of the population system, i.e., I_1. Let $N^d = \sum_{i=1}^{14} N_i^d$ be the total number of deaths over all groups, with N_i^d the number of deaths within group i. Intuitively, the global number of births, I_1, is

$$I_1 := \dot{N} + N^d.$$

Once the number of births is computed, it is easy to obtain the population transfer from group 1 into group 2, $T_{1,2}$, as

$$T_{1,2} := I_1 - \dot{N}_1 - N_1^d.$$

Therefore, we identify Eq. 1 for the dynamics of the age group N_1 to be

$$\dot{N}_1 = I_1 - \underbrace{O_1}_{=T_{1,2}+N_1^d}.$$

The logic is similar for groups $N_2, \ldots, N_{13}$ when identifying $I_i := T_{i-1,i}$, and $O_i := T_{i,i+1} + N_i^d$. As expected, the last cohort's outflow is only characterized by $O_{14} := N_{14}^d$. Therefore, we are able to determine each variable of Eq. 1 for the fourteen age groups, and consequently we can compute the global population N.[9]

2.2 Determining parametric forms for the birth and death rates

Inflows and outflows in our model are defined by 15 dynamic variables: (i) the birth rate determining the inflow in the first age group, I_1, (ii) the fourteen specific death rates of any i^{th} age group

[9]Logically, the transfered population of a given group, $T_{i,i+1}$, should be strictly equal to the population number of the next group after taking into account the number of deaths, $N_{i+1} - N_{i+1}^d$. However, we observed in the data a mismatch between those variables. We argue that this discrepancy comes from the fact that death numbers in each 5-year age groups are estimated every five years by the UN *from mid-year to mid-year*.

allowing a distinction between aging and death outflows. According to the literature, the birth rate depends on various determinants, such as, education (Becker et al., 2010; Murphy, 2015), demand for human capital (Galor and Mountford, 2008; Greenwood and Seshadri, 2002), secularization (Peri-Rotem, 2016), marriage patterns (Carmichael et al., 2016), women empowerment (Diebolt and Perrin, 2013; Murphy, 2015), and wealth inequalities (Cummins, 2013). Similarly, death rates vary according to many different variables, such as the level and quality of nutrition (De Onis, 2000), reductions in contagious and infectious diseases through personal hygiene and public health measures (Luby, 2017), reductions in chronic and degenerative diseases (Lee, 2003, p. 171), air pollution (Di et al., 2017), and the frequency of armed conflict (Guha-Sapir and van Panhuis, 2003).

The aim of this paper is to provide a simple world demographic dynamics model that could be included in IAMs. We chose *per capita gross world product* (with GWP retrieved from the World Bank (2018)) as the exclusive correlative (and not explanatory) variable for the birth rate and for the evolution of age-specific death rates. Notwithstanding the well-known drawbacks surrounding GWP (hereafter Y) as an indicator of wealth (or prosperity), we argue below that this indicator remains a good proxy for the explanatory factors listed *supra* in determining the evolution of the birth and death rates.[10]. Thus, the approach proposed here is *phenomenological* (rather than micro-funded), because it relies on relations that emerged from data observed at the global long-term scale.

2.2.1 Global birth rate as a function of GWP per capita

Figure 3 shows the scatter plot of the global birth rate and GWP per capita. It displays a S-shaped relationship between the two variables. Therefore, we model the evolution of the global birth rate, $BR := I_1/C_2$, as a sigmoid function of per capita GWP, Y/N.

$$BR := \overline{BR} + \frac{\underline{BR} - \overline{BR}}{(1 + \exp(-\delta(Y/N - \phi)))^{\frac{1}{\nu}}} \tag{2}$$

where $\overline{BR}$ and $\underline{BR}$ respectively represent the upper and lower asymptotes, δ is a slope parameter, ϕ is the inflection point, and ν is a parameter that controls the curvature of the function near the asymptotes.

Figure 3 also displays the result obtained from minimizing the sum of squared errors between the historical data (black dots) and the model of Eq. 2 (blue line).[11] Best-fit values of parameters are reported in Table 2. As can be seen, the high asymptote of 0.39 births per young active individual (i.e, 15–49 years old) every five years is about twice as high as the low asymptotic of 0.18 births per young active individual every five years.

Table 2: Best-fit parameters of the global birth rate sigmoid function.

$\overline{\mathbf{BR}}$	$\underline{\mathbf{BR}}$	δ	ϕ	ν
0.39	0.18	0.00087	4033.6	0.18

[10]Regarding birth, our approach is in line with Becker (1960) who suggests that the rise in income induces a fertility decline, because the positive income effect on fertility is dominated by a negative substitution effect induced by the rising opportunity cost of raising children

[11]The minimization procedure consists in findings the parameters that minimize the sum of squared residuals. In practice, we selected the model that minimizes a BFGS algorithm employed with various initial points. More details are available upon request.

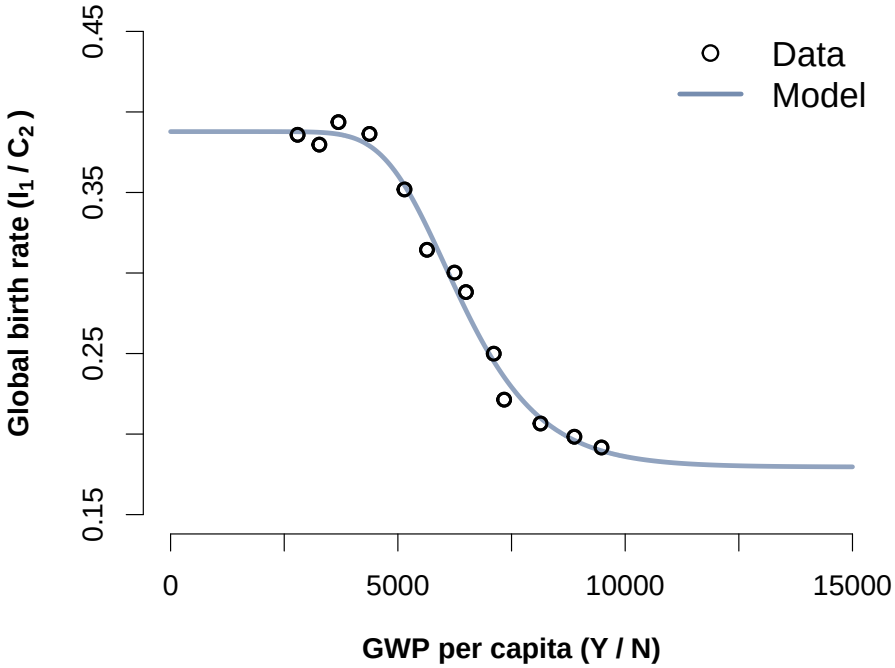

Figure 3: Global birth rate as a function of per capita GWP.

2.2.2 Age-specific global death rates as functions of per capita GWP

We also observed a robust decreasing relationship between the global death rate of every age group and the GWP per capita. However, depending on the age group, the functional relationship can be either exponential or sigmoid. We choose to model the evolution of the different global death rates, $DR_i := N_i^d/N_i$, as decreasing sigmoid functions of GWP per capita, Y/N, for two reasons. First, the sigmoid function is a more general formulation of the exponential. But mostly, an exponential relationship would imply that death rates tend towards infinity as per capita GWP tends towards zero. Such an assumption would not make sense because an individual surviving alone on an island would certainly have a non-infinite death rate even though the economic system he is living in would match the description of a 'zero GDP' economy.

$$DR_i = \overline{DR_i} + \frac{\underline{DR_i} - \overline{DR_i}}{(1 + \exp(-\delta_i(Y/N - \phi_i)))^{\frac{1}{\nu_i}}} \tag{3}$$

where, for any age group i, $\overline{DR_i}$ and $\underline{DR_i}$ respectively represent the upper and lower asymptotes, δ_i is a slope parameter, ϕ_i represents the inflection point, and ν_i is a parameter controlling for/that controls the curvature of the function near the asymptotes.

Figure 4, 5, 6, and 7 show the results of the minimization procedure (defined *supra*) for Eq. 3. Best-fit values of parameters are reported in Table 3. In terms of orders of magnitude, the N_1 group of 0–4 year-olds is very distinguishable since its upper asymptote is twice as large as those of groups N_2 to N_{13}. The N_{14} group of over 65 year-olds is also discernible as part of the fragile population.

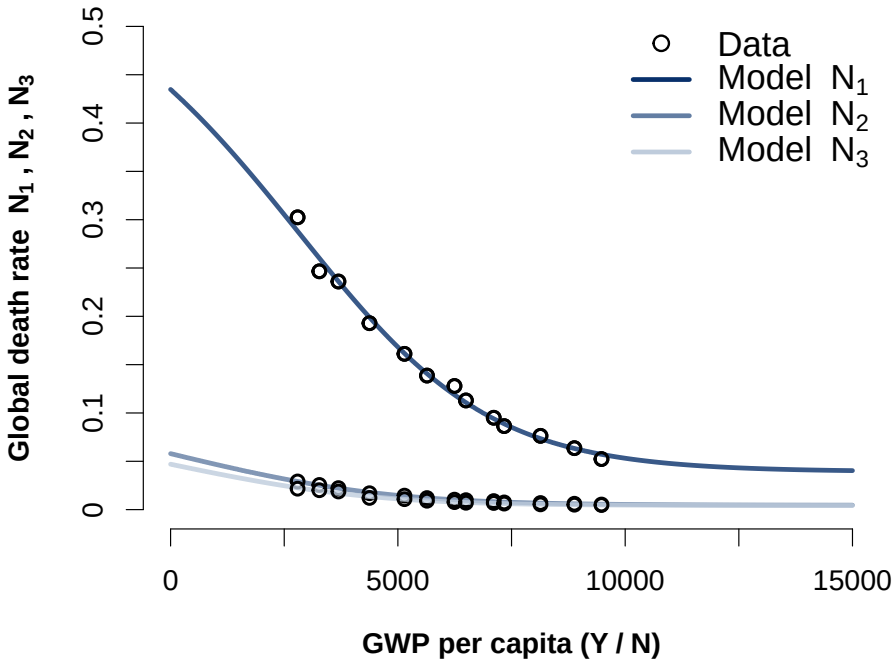

Figure 4: Global death rates for cohort C_1 (groups N_1 to N_3) as functions of per capita GWP.

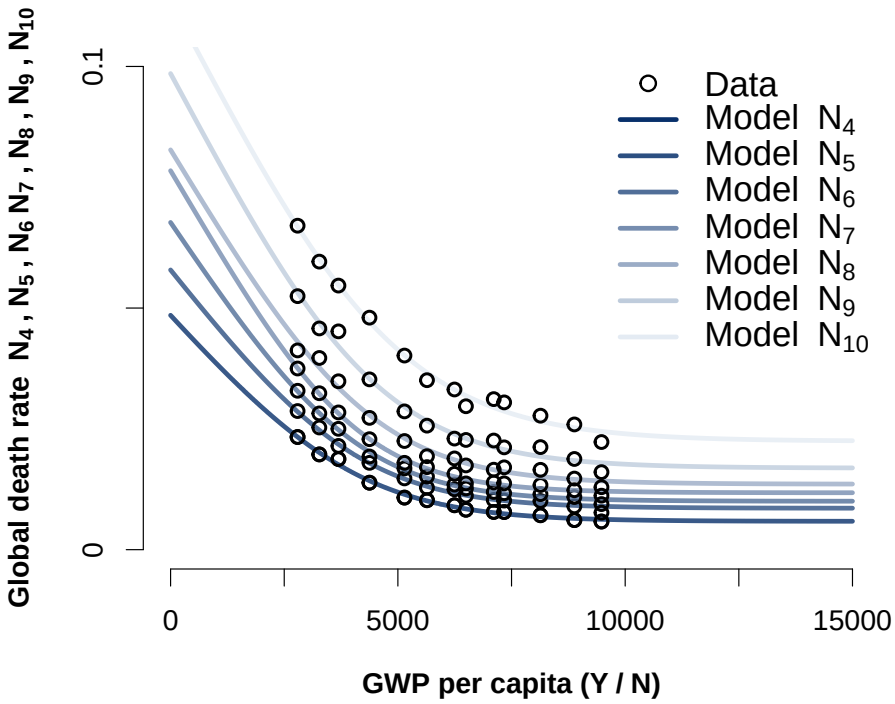

Figure 5: Global death rates for cohort C_2 (groups N_4 to N_{10}) as functions of per capita GWP.

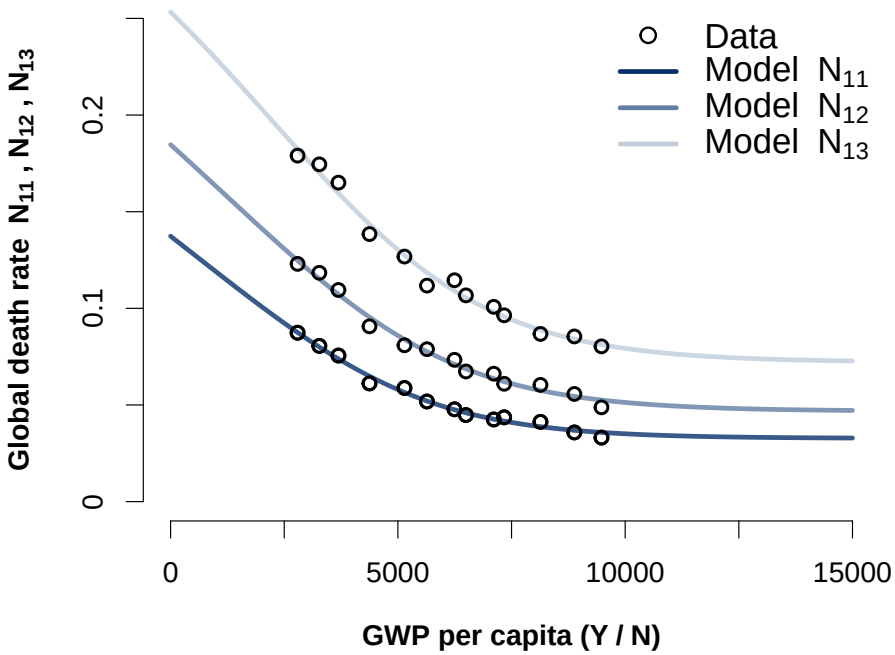

Figure 6: Global death rates for cohort C_3 (groups N_{11} to N_{13}) as functions of per capita GWP.

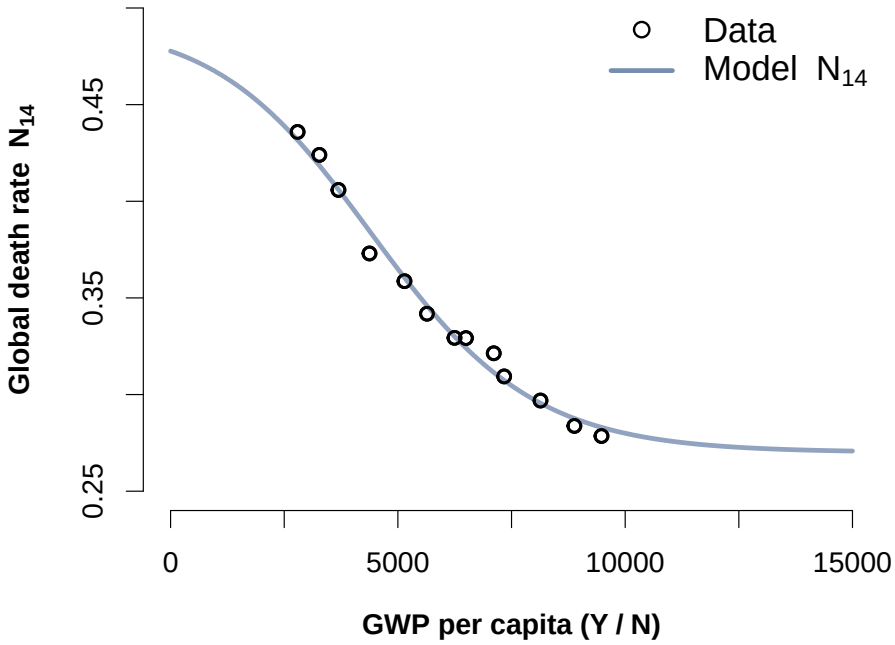

Figure 7: Global death rate for cohort C_4 (group N_{14}) as a function of per capita GWP.

Table 3: Best-fit parameters of the global death rate sigmoid function for each 5-year age group.

Age group	$\overline{\mathbf{DR_i}}$	$\underline{\mathbf{DR_i}}$	$\delta_\mathbf{i}$	$\phi_\mathbf{i}$	$\nu_\mathbf{i}$
N_1	0.60192	0.0392421	0.00051169	3951.5	1.76828
N_2	0.34980	0.0045840	0.00054322	3441.8	11.99152
N_3	0.33501	0.0042607	0.00058728	3312.8	15.02963
N_4	0.33232	0.0058662	0.00063047	3282.7	15.63468
N_5	0.33982	0.0085766	0.00066358	3364.8	14.48400
N_6	0.34346	0.0100244	0.00069397	3323.4	12.63958
N_7	0.32770	0.0117765	0.00072698	3297.5	10.48483
N_8	0.35451	0.0135612	0.00064659	3469.5	10.33744
N_9	0.34216	0.0168843	0.00060129	3365.7	7.43185
N_{10}	0.35791	0.0224452	0.00054379	3601.1	6.59593
N_{11}	0.38159	0.0327278	0.00052461	4018.9	6.23736
N_{12}	0.39385	0.0467704	0.00048987	4187.2	4.28997
N_{13}	0.39473	0.0721157	0.00048556	4246.3	2.64664
N_{14}	0.49206	0.2701185	0.00054744	4104.9	0.85705

2.3 Theoretical model and its properties

We now turn to the presentation of our theoretical model and the analysis of its equilibrium properties. Recall that the unit time between consecutive periods (t and $t+1$) corresponds to the number of years during which individuals remain in a given age-group (i.e., 5 years in the UN data presented in the previous section). Therefore, the outflow of population among age groups $i \in \{1, \ldots, 13\}$ will be the entire population in each group. For each of these outflows, the population that survived remains in the system. This share of population for a given age-group i is represented by $DR_i^* := 1 - DR_i$. Let $\overrightarrow{N}$ be the column vector of all the age groups. The theoretical model is linear and can be written as

$$\dot{\overrightarrow{N}} = A\overrightarrow{N},$$

where the A matrix is explicitly provided in System 4.

$$
\begin{pmatrix} \dot{N}_1 \\ \dot{N}_2 \\ \dot{N}_3 \\ \dot{N}_4 \\ \dot{N}_5 \\ \dot{N}_6 \\ \dot{N}_7 \\ \dot{N}_8 \\ \dot{N}_9 \\ \dot{N}_{10} \\ \dot{N}_{11} \\ \dot{N}_{12} \\ \dot{N}_{13} \\ \dot{N}_{14} \end{pmatrix}
=
\underbrace{\begin{pmatrix}
-1 & 0 & 0 & BR & BR & BR & BR & BR & BR & BR & 0 & 0 & 0 & 0 \\
DR_1^* & -1 & 0 & 0 & 0 & 0 & 0 & 0 & 0 & 0 & 0 & 0 & 0 & 0 \\
0 & DR_2^* & -1 & 0 & 0 & 0 & 0 & 0 & 0 & 0 & 0 & 0 & 0 & 0 \\
0 & 0 & DR_3^* & -1 & 0 & 0 & 0 & 0 & 0 & 0 & 0 & 0 & 0 & 0 \\
0 & 0 & 0 & DR_4^* & -1 & 0 & 0 & 0 & 0 & 0 & 0 & 0 & 0 & 0 \\
0 & 0 & 0 & 0 & DR_5^* & -1 & 0 & 0 & 0 & 0 & 0 & 0 & 0 & 0 \\
0 & 0 & 0 & 0 & 0 & DR_6^* & -1 & 0 & 0 & 0 & 0 & 0 & 0 & 0 \\
0 & 0 & 0 & 0 & 0 & 0 & DR_7^* & -1 & 0 & 0 & 0 & 0 & 0 & 0 \\
0 & 0 & 0 & 0 & 0 & 0 & 0 & DR_8^* & -1 & 0 & 0 & 0 & 0 & 0 \\
0 & 0 & 0 & 0 & 0 & 0 & 0 & 0 & DR_9^* & -1 & 0 & 0 & 0 & 0 \\
0 & 0 & 0 & 0 & 0 & 0 & 0 & 0 & 0 & DR_{10}^* & -1 & 0 & 0 & 0 \\
0 & 0 & 0 & 0 & 0 & 0 & 0 & 0 & 0 & 0 & DR_{11}^* & -1 & 0 & 0 \\
0 & 0 & 0 & 0 & 0 & 0 & 0 & 0 & 0 & 0 & 0 & DR_{12}^* & -1 & 0 \\
0 & 0 & 0 & 0 & 0 & 0 & 0 & 0 & 0 & 0 & 0 & 0 & DR_{13}^* & -DR_{14}
\end{pmatrix}}_{=:A}
\begin{pmatrix} N_1 \\ N_2 \\ N_3 \\ N_4 \\ N_5 \\ N_6 \\ N_7 \\ N_8 \\ N_9 \\ N_{10} \\ N_{11} \\ N_{12} \\ N_{13} \\ N_{14} \end{pmatrix}
\tag{4}
$$

Turning to the equilibrium properties of System 4, we focus on the analysis of the A matrix. As the dimensionality of matrix A is relatively high, let us first consider a lower dimensional system that may be more easily understood. Using M instead of N, we consider the following three-dimensional system

$$\begin{pmatrix} \dot{M}_1 \\ \dot{M}_2 \\ \dot{M}_3 \end{pmatrix} = \underbrace{\begin{pmatrix} -1 & BR & 0 \\ 1-DR_1 & -1 & 0 \\ 0 & (1-DR_2) & -DR_3 \end{pmatrix}}_{=:B} \begin{pmatrix} M_1 \\ M_2 \\ M_3 \end{pmatrix} \tag{5}$$

System 5 has one obvious equilibrium point, $(0,0,0)$. Its local asymptotic stability will depend on whether the linear matrix, B, is a negative-definite matrix. The second obvious equilibrium is $(+\infty,+\infty,+\infty)$ retrieved from the change of variable $(1/M_1, 1/M_2, 1/M_3)$. Its local asymptotic stability will depend on whether the linear matrix, $-B$, is a negative-definite matrix. The third (set of) equilibria comes under very specific conditions: (i) $(1-DR_1)BR = 1$; and (ii) $M_3 = (1-DR_2)/(DR_3)M_2 = (1-DR_2)/(BR \times DR_3)M_1$. Condition (i) implies that the determinant of the matrix B, $\det(B) = -DR_3(1-BR(1-DR_1))$ equals zero, which would make this set of equilibria structurally unstable. Therefore, the system is asymptotically unstable in the sense that there is no stable equilibrium besides zero or infinity, under specific specifications.

Interestingly, when computing the determinant of the full system, we find a result that is akin to the determinant of the B matrix,

$$\det(A) = DR_{14}\left[1 - BR\sum_{i=3}^{9}\prod_{j=1}^{i} DR_j^*\right].$$

As $BR < 1$ and $DR_i < 0\ \forall i$, $\det(A) \neq 0$[12] and, therefore, no finite positive equilibrium can be found.[13] Therefore, the model we designed in the present article would not be suitable for the debate on the global carrying capacity. However, we believe that our model is a useful tool for short- and even medium-term simulation purposes, as illustrated by its robustness to the historical analysis presented in the following section.

3 Simulation: historical fit and projections under exogenous GWP scenarios

In the present section, we perform three simulation runs: (i) an assessment of the historical performance of our model; (ii) an appraisal of the model's prospective behavior under four different exogenous GWP trajectories, (iii) an extension of the former approach with the addition of exogenous climate change. For all simulations, the unit of time–between t and $t+1$—is 5 years.

3.1 Historical fit

To assess the empirical robustness of our model, we present the results from its back-testing analysis over the last century. Using values from Table 2 and Table 3, we ran our world population model from 1950 onward with the historical GWP per capita already used in Section 2.[14] Figure

[12] Except for a very particular combination of variables that we do not have in our analysis and calibration.

[13] Moreover, we note that under the suggested calibration, numerical simulations of the A matrix show that only one eigenvalue remains positive for all levels of GWP per capita. This makes System 4 asymptotically unstable.

[14] We did not perform a historical fit further back because of the lack of reliable estimates of GWP/capita prior 1950 (for example some available years are 1940, 1913, 1870, and 1820 from Bolt et al. (2013)). It is worth noting that the

8 shows that the back-testing simulation is excellent for the first ten periods of time (1950–2000), after which the model starts to slightly underestimate the actual historical population. The initial underestimation in 2000 worsened up until 2015 due to accumulated errors. A comparison of the real data age structure in 2015 with the model output made in Figure 9 shows that the overall underestimation of the model is due to a 0.06 billion overestimation for group N_{14} (65+ years-old) that is more than compensated by a 0.05 billion underestimation for group N_6 (25–29), a 0.04 billion underestimation for group N_{10} (45–49), a 0.03 billion underestimation for group N_9 (40–44), a 0.02 billion underestimation for groups N_2 (5–9), N_5 (20–24), N_7 (30–34), and N_{11} (50–54), and to a lesser extent, a 0.01 billion underestimation for groups N_1 (0–4) and N_3 (10–14).

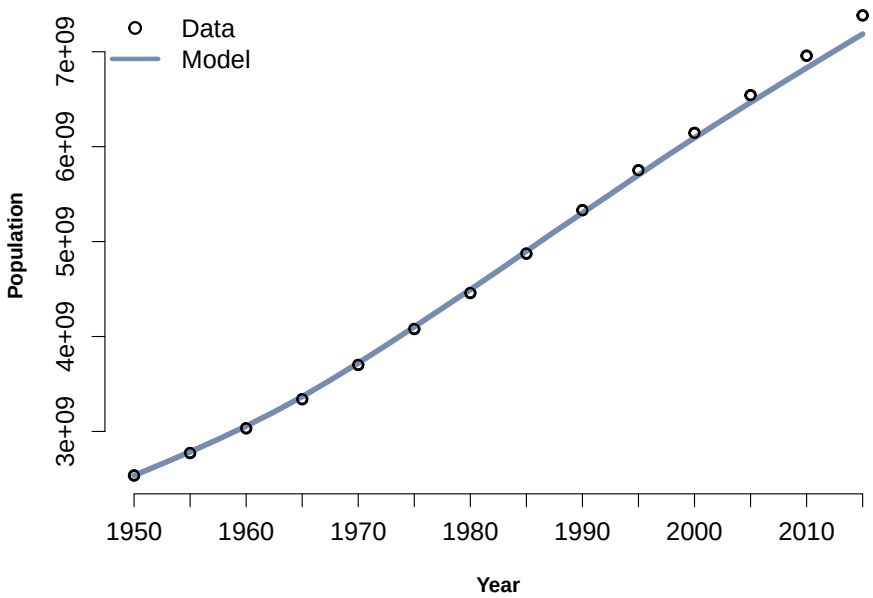

Figure 8: Historical vs. back-tested simulation of the world population, 1950–2015.

rare GWP/capita estimates prior 1950 are the subject of continuing debates (e.g. Jerven (2012), Prados de la Escosura (2016)). Moreover, to comply with our framework, it would be necessary to carry out precarious interpolations to obtain GWP/capita estimates with a 5-year interval. For these two reasons, we restrict the model estimation to the post-WWII period.

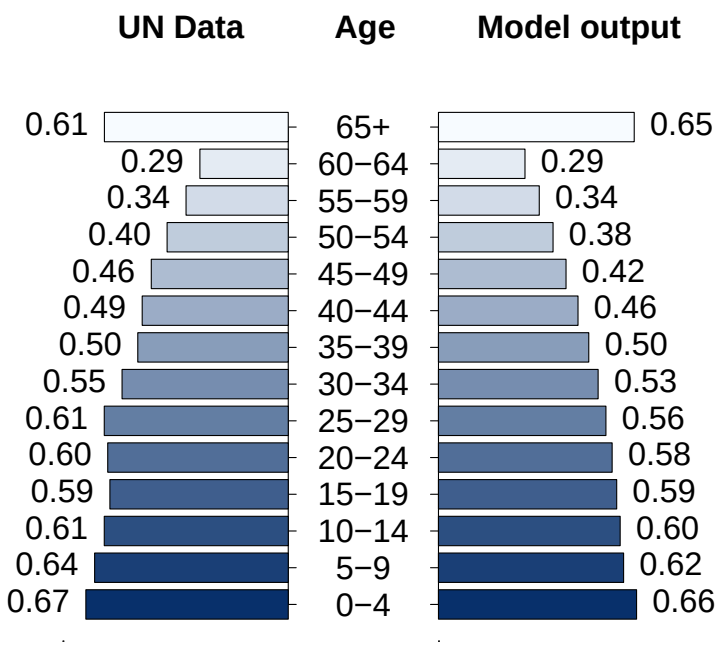

Figure 9: UN data vs. model output population pyramids in 2015 (in billions).

3.2 Population projections under exogenous GWP scenarios

To analyze the sensitivity of our model to the GWP per capita input, we suggest four prospective scenarios for the exogenous GWP per capita trajectory. We use the first three Shared Socioeconomic Pathways (SSP) developed for the last report from the Working Group III of IPCC (2014), in addition to a fourth scenario we called *Collapse*.

- *SSP1* – Taking the Green Road (Low challenges to mitigation and adaptation): The world shifts gradually, but pervasively, towards a more sustainable path, emphasizing more inclusive development that respects perceived environmental boundaries, triggering a large scale learning effect and positive externalities that boost growth relative to the business-as-usual (i.e., *SSP2*) scenario.
- *SSP2* – Middle of the Road (Medium challenges to mitigation and adaptation): The world follows a path in which social, economic, and technological trends do not shift markedly from historical patterns. This is the business-as-usual scenario.
- *SSP3* – A Rocky Road (High challenges to mitigation and adaptation): Resurgent nationalism, concerns about competitiveness and security, and regional conflicts push countries to increasingly focus on domestic or at most, regional issues, which results in a lower GWP trajectory than the business-as-usual (i.e., *SSP2*) scenario.
- *Collapse* – Going Down the Slope (Abrupt economic collapse in the middle of the twenty-first century): assumes the *SSP2* scenario until 2050, then over five years GWP linearly decreases to one half of the GWP in 2015, because of an assumed major financial or environmental crisis.

The SSP scenarios already contain population trajectories that we are not going to use as inputs, but that are worth describing. Figure 10 shows that the population assumed in *SSP1* is really closed

to the UN low variant, whereas population in *SSP2* (respectively *SSP3*) lies in between the UN medium and low (medium and low) variants. Figure 11 gives a visual representation of the four exogenous GWP trajectories that we used as inputs for our world population model, while Figure 12 and Figure 13 show the simulation results.

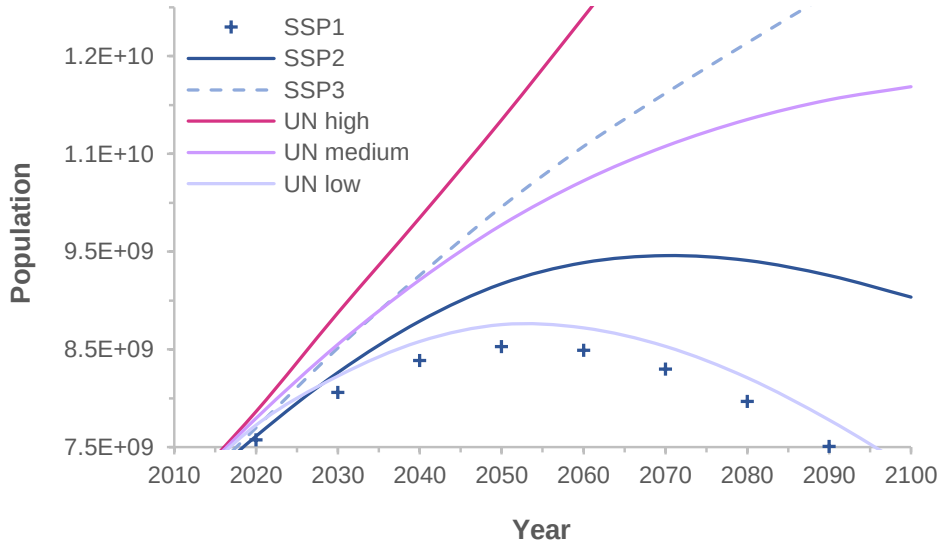

Figure 10: Original population trajectories of SSP scenarios compared to three United Nations variants, 2015–2100.

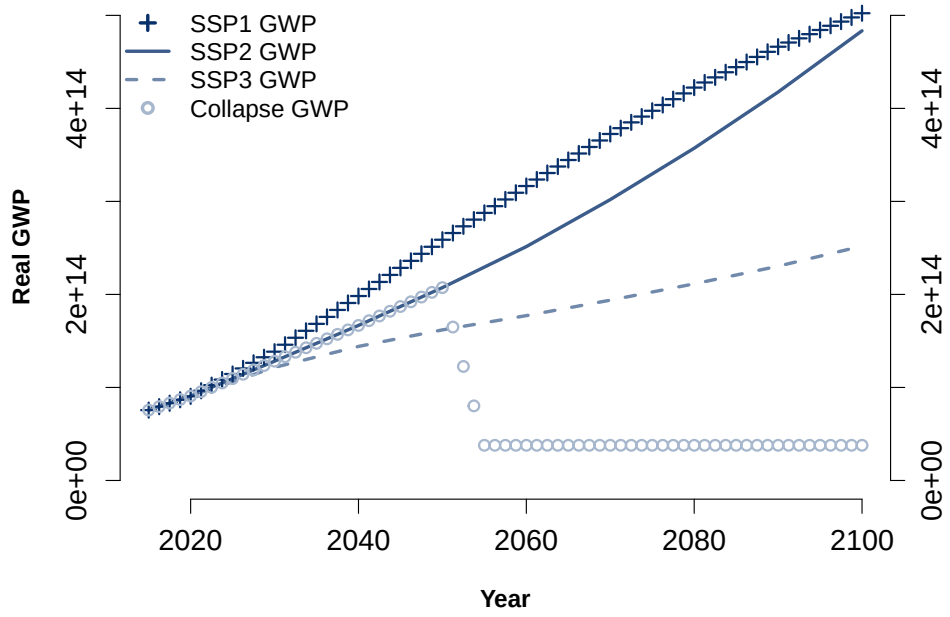

Figure 11: Four scenarios of exogenous GWP, 2015–2100.

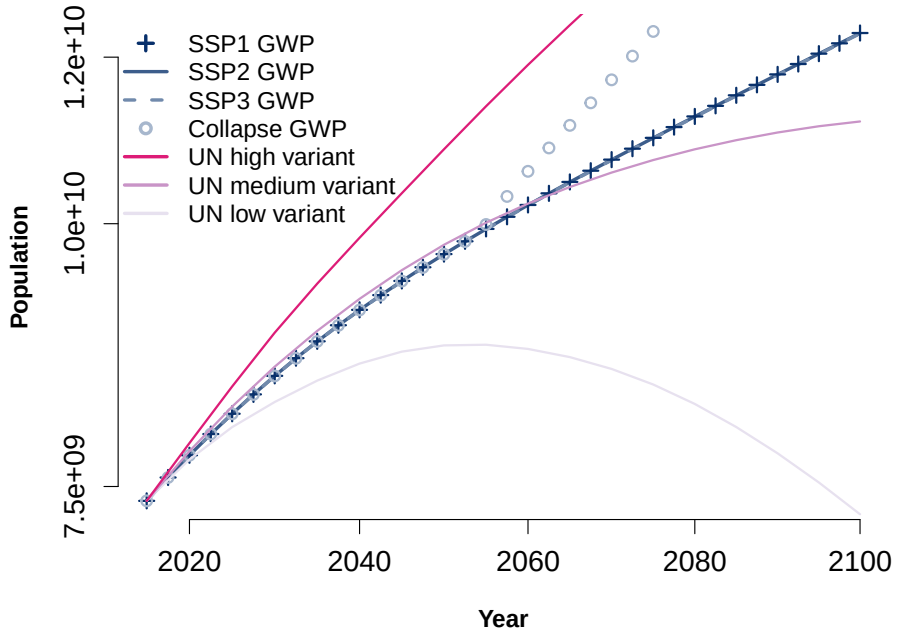

Figure 12: Global population projections of the model for the four exogenous GWP scenarios compared to three United Nations variants, 2015–2100.

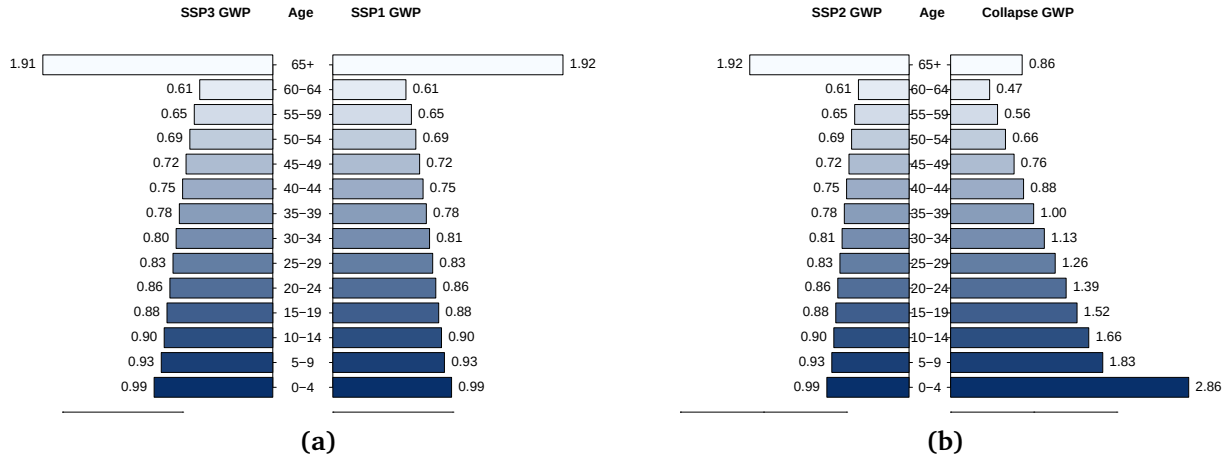

Figure 13: Population pyramids in 2100 for the four prospective scenarios (population in billions).

The most striking result from our simulation is that given the significant differences between the GWP input of the three SSP scenarios, and contrary to the original population trajectories embedded in these scenarios (Figure 10), there is notable consistency in the population dynamics delivered by our model for the *SSP1 GWP*, *SSP2 GWP*, and *SSP3 GWP* scenarios. Simulations under the three different exogenous GWP from SSP scenarios are indeed extremely similar and very close to the United Nations medium projection up to 2065, after which date they are clearly above. This means that in the low and medium variants of the UN population model, fertility rates decrease far more rapidly after 2065 than in the previous decades of the twenty-first century.

Given our model, this behavior makes perfectly sense. Indeed, although we consider different

exogenous GWP dynamics in each of the three SSP scenarios, all of them consider GWP levels that are above the 2015 level. Hence, in all our simulations using the GWP from one of the three SSPs, prevailing birth rate and death rates correspond to the lower asymptotic limits from Figures 3 to 7.[15]

Our simulation results yield two major implication. First, the SSP scenarios developed for the last IPCC (2014) report of Working Group III take no account of the historical relationship that prevailed between GWP and population from 1950 to 2015. In other words, the population trajectories assumed in SSP scenarios (shown in Figure 10) are uncorrelated to the GWP trajectories of these same scenarios. Second, the low and even medium prospective variants of the United Nations also assume future decoupling possibilities between economic development and fertility that have never been witnessed during the last sixty-five years.

The *Collapse GWP* scenario yields very different results in comparison with the outputs of the three SSP scenarios, with increasingly divergent population dynamics. The age structure of the population in the *Collapse* GWP simulation is significantly different from the three SSP scenarios. The abrupt collapse implies that the birth rate increases relative to the death rates so that the overall population grows and gets younger. As illustrated in Figure 14, this difference in age structure is important in terms of active population size and labor force availability. Indeed, in 2075 (2100 respectively) the active population is 6 (4.4) percentage points lower in the *Collapse* simulation relative to the *SSP2* scenario. The result of the *Collapse* scenario may appear counter-intuitive to some readers who would more willingly imagine a sharp decrease in the population level as, for instance, in the *World3* model of Meadows et al. (1972). However, in the *World3* model it is the over-exploitation of non-renewable resources, together with the resulting unsustainable levels of pollution, that leads to a decrease in soil fertility and, consequently, to a decrease in agricultural production, and a subsequent decrease in population. Conversely, in the present paper we are not modelling agricultural production, but rather are pointing out that given the relationships that have prevailed for the past 65 years between the GWP per capita on the one hand, and birth and death rates on the other hand, a *Collapse* scenario implies an increase and not a decrease in the world population.

That being said, because our model was calibrated on historical ever-increasing GWP, we can be more confident in the output it delivers under prospective ever-increasing GWP trajectories (such as the three *SSP* scenarios) than under the *Collapse* trajectory. Indeed, so far, we did not focus on the robustness of our model in the context of a long-lasting economic degrowth. Moreover, if our human population model is to be included in IAMs, the impacts of climate change on the population dynamics should also be considered. As discussed in the following section, economic collapse and climate change constitute two (possibly associated) regime changes that may imply some refinements of our world population model.

[15] Another sensitivity analysis of the model under scenario *SSP2* is provided in Appendix A using *ad-hoc* birth and death rates.

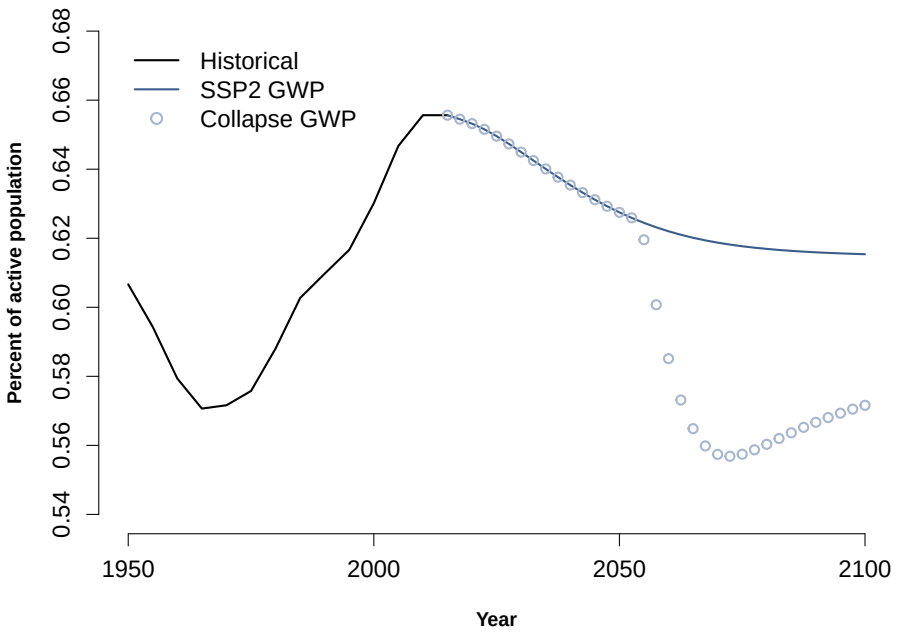

Figure 14: Percent of active population: historical, *SSP2* and *Collapse* GWP scenarios.

4 Discussion: economic degrowth and climate change

In this section, we discuss two possible refinements of our model, namely the impact on birth and deaths rates of (i) economic degrowth events, and (ii) climate change.

4.1 Investigating regime change under economic degrowth

In order to assess the possibility of introducing asymmetry into our model with an economic degrowth regime, we review the historical impacts of past economic recessions on birth and death rates.

4.1.1 The impact of economic recessions on birth rates

Although our model takes a global perspective, we investigated the impact of recessions at the country level. We are well aware of the potentially spurious conclusions that can arise when mixing assessments of such disparate scales (e.g., aggregation problem, emergence phenomenon). However, we are limited by the lack of global observations on the effects of deep economic recessions.

The literature is not unanimous on the impact of economic recessions on fertility. However, most studies suggest that fertility trends often react pro-cyclically, with delays. Hence, periods of economic recession (or stagnation) are frequently followed within one or two years by a decline in birth rates. However, Sobotka et al. (2011) stress that these cyclical waves are usually short and relatively small (a few percentage points). The change can therefore be overshadowed by long-term secular trends in fertility caused by factors other than economic recession. This observation explains why a number of studies on fertility during the Great Depression of the 1930s–and other major recessionary events–found no statistically significant relationship between the recession and the changes in birth rates. Both periods showed consistent long-term fertility declines that started well before recessionary events (Table 4). Therefore, it is impossible to attribute a declining fertility

trend to the recession itself, because in all countries under consideration in Table 4, birth rates were on long-term declining trends prior to degrowth episodes.

Table 4: Impacts of economic recessions on birth rate (BR) and death rate (DR).

Country (recession time period)	**Avg. GDP/capita** decline **during recession (%/yr)**	**Avg. change of BR before/ during/after recession (%/yr)**	**Avg. change of DR before/ during/after recession (%/yr)**
Germany (1929—1932)	-4.7	-0.3 / -5.0 / 0.4	-3.1 / -1.5 / 1.1
USA (1930—1933)	-8.8	-3.2 / -2.7 / -0.2	? / -2.5 / 1.8
Chile (1972–1975)	-6.2	-2.1 / -3.1 / -1.0	-2.7 / -3.5 / -2.6
Peru (1976–1978)	-2.2	-1.5 / -1.5 / -1.9	-3.5 / -3.2 / -3.3
Peru (1988–1992)	-10.4	-1.9 / -1.8 / -2.2	-3.3 / -2.6 / -2.1
Argentina (1988–1990)	-4.1	-1.3 / -0.7 / -1.3	-0.6 / -0.5 / -0.6
Argentina (1999–2002)	-5.9	-1.3 / -0.7 / -0.7	-0.6 / -0.2 / -0.2
Mexico (1986–1988)	-2.1	-2.8 / -1.5 / -1.6	-3.3 / -2.0 / -1.7
Russia (1990–1996)	-7.4	-0.7 / -6.7 / 1.6	-0.0 / 4.4 / 0.8
Bulgaria (1990–1998)	-1.2	-1.9 / -5.0 / 2.3	1.2 / 2.0 / 0.4
Bulgaria (1999–2015)	-0.8	-4.8 / -4.6 / ?	1.8 / -5.1 / ?
Zimbabwe (1999-2008)	-6.6	-1.5 / 0.6 / -0.7	5.2 / -0.9 / -6.8
Greece (2007–2013)	-4.8	1.2 / -2.5 / -1.2	0.8 / 0.5 / 4.8
Venezuela (2014–2016)	-10.5	-1.4 / -1.5 / ?	0.9 / 0.8 / ?

Note: when data is available, average change of birth rate (respectively death rate) before and after a recessionary episode are calculated for the ten previous (respectively following) years.

4.1.2 The impact of economic recessions on death rates

A significant corpus of articles shows that in developed countries general mortality and age-specific death rates tend to increase during economic expansions and decrease during recessions for both males and females–although the effect is more apparent for males. Hence, Tapia Granados and Diez Roux (2009) found that population health actually improved during the four years of the US Great Depression (1930–1933) with decreases in mortality for almost all ages, and increases of several years in life expectancy for both males and females, and whites and nonwhites. Similarly, Tapia Granados and Ionides (2017) show that in the European countries in which the Great Recession of 2007-2008 was particularly severe, mortality reductions in 2007–2010 were considerably larger than in 2004–2007. Broadly speaking, these studies find that during episodes of economic crises, deaths due to infectious disease and transport accidents tend to decrease, while deaths caused by diabetes, hypertensive disease, chronic poisoning (alcohol, tobacco), and suicide tend to increase increase to a lesser extent. The result is a decrease in the aggregate death rate. In other words, in these examples, the detrimental effect of recessions on health is not important enough to revert the accumulated progress of the health system. However, the dissolution of the Soviet Union offers a counter-example of countries facing prolonged economic degrowth associated with an increased death rate (see Shkolnikov et al. (2001) for Russia, and Carlson and Tsvetarsky (2000) for Bulgaria). As summarized in Table 4, evidence suggests that the economic recessions must be severe enough, and associated with a (partial) collapse of political institutions, in order to observe an increase in the death rate during (for former USSR countries) or just after (for Greece, Germany, and possibly Venezuela) the economic crisis. If political institutions are not too severely disturbed during recessions, such that material needs and health infrastructures hold, then death rates seem to stay on their declining pace (Argentina, Mexico, USA, Peru, Chile, Zimbabwe).

In summary, it seems warranted to consider that it is the *level* of GWP per capita, rather than its upward or downward *change*, that determine both the birth rate and death rates of population. As a consequence, the global population model presented in Section 2 does not require further

adjustment.

4.2 Excess mortality function associated with climate change

Most IAMs take into account the impacts of climate change through a damage function on production, capital, or productivity (Diaz and Moore, 2018; Tol, 2018), while the population dynamics follow an exogenous trend. We argue that endogenizing the population dynamics would require a distinct damage function that would include the idiosyncratic effect of climate change on human health.

4.2.1 Framework

Climate change affects human health in four principal ways, namely, (i) increased undernutrition due to decreases in crop yields, and increased malnutrition due to changes in the macro- and micro-nutrients contents of cereals (Smith and Myers, 2018; Springmann et al., 2016), (ii) altered distribution of allergens and vector-borne infectious diseases resulting in higher risk of typhus, cholera, malaria, dengue, and West Nile virus infection (Franchini and Mannucci, 2015), (iii) increased prevalence of diarrhoeal diseases due to more frequent and longer drought periods causing reduced safe water availability (Kolstad and Johansson, 2011), and (iv) increased frequency of heat waves that translates into higher mortality related to acute and chronic respiratory, or cardiovascular diseases (Mora et al., 2017).[16]

The 2014 assessment performed by the World Health Organization (WHO, 2014) is, to the best of our knowledge, the only study estimating the total number of additional deaths that can be attributed to climate change at the global scale. The assessment uses an IPCC's (2000) A1b scenario, for 2030 and 2050, and for five mortality risks: undernutrition (for children under 5), malaria (for all ages), dengue (for all ages), diarrhoeal diseases (for children under 15), and heat waves (for people above 65). As shown in Table 5, for undernutrition, malaria, and diarrhoeal diseases, the global additional number of deaths estimated in the WHO (2014) study are higher in 2030 than in 2050. This counter-intuitive result is due to the assumed adaptation of population to climate-induced mortality risks; however, assumed adaptation is not sufficient to prevent an increase in heat-related and dengue-related deaths between 2030 and 2050.

Table 5: Global additional deaths in 2030 and 2050 attributable to climate change for five mortality risks. Source: WHO (2014, p. 7 and p. 12, respectively).

	Undernutrition	Malaria	Dengue	Diarrhoeal diseases	Heat waves	Total
Global additional deaths in 2030	95,176 (-119,807 to 310,156)	60,091 (37,608 to 117,001)	258 (136 to 331)	48,114 (21,097 to 67,702)	37,588 (26,912 to 48,390)	241,227 (-34,054 to 543,580)
Global additional deaths in 2050	84,697 (-29,203 to 163,989)	32,695 (22,786 to 40,817)	282 (195 to 342)	32,955 (14,914 to 49,151)	94,621 (70,775 to 126,684)	245,250 (79,467 to 380,983)

Note: the central estimate is the mean, based on three scenarios used with three different global climate models for a total of five runs. The uncertainty interval in brackets is the lowest and highest estimates, except for undernutrition where the uncertainty interval is mean ± 1 standard deviation of the probability density function.

As far as we are aware, Pottier et al. (2018) have suggested the first excess mortality function associated with climate change. In their framework, each of the five climate-induced mortality risks identified in the WHO (2014) study constitutes an element j among the set $J = \{\text{Undernutrition}, \text{Malaria},$

[16] At mid latitudes increasing temperature may reduce the rate of diseases related to cold temperatures (such as pneumonia, bronchitis and arthritis), but these benefits are unlikely to counterbalance the global risks associated with warming that low latitudes regions will suffer the most (Gasparrini et al., 2017).

Dengue, Diarrhoeal diseases, Heat waves}. As shown in Eq. 6, the excess mortality function associated with climate change consists of a multiplier that increases the specific death rate of any age-group i in the population model,

$$\widetilde{DR}_i = DR_i \underbrace{\left[1 + \sum_{j \in J} \alpha_{i,j} \left(\frac{T}{T^0}\right)^{\theta}\right]}_{\text{Climate change induced multiplier}} . \tag{6}$$

Where $\alpha_{i,j}$ is the relative increase in the probability of dying due to risk j for the age-group i at the calibration temperature increase T^0 (i.e., the temperature change of +2.5°C in 2050 for the A1b scenario used in the WHO (2014) study), T is the prevailing global temperature change (also called temperature anomaly) relatively to the pre-industrial era, and parameter θ specifies the dependence of the probability of dying with respect to temperature.

As discussed in Pottier et al.'s (2018) article, four main assumptions are embedded in the choice of the functional form of Eq. 6. First, the climate-induced death rates are multiplied by the death rate without climate change. This is a reasonable assumption, since climate-induced mortality will certainly be influenced by general sanitary conditions, health systems, and the availability of pharmaceutical drugs, which are all factors that are already reflected in the evolution of the DR_i over time. Second, the different j risks do not equivalently affect the different i age-groups as we follow the WHO (2014) classification (e.g., malaria affects all age groups, whereas diarrhoeal diseases only affect children under 15). However, the overall number of additional deaths associated with a given climate-induced risk j are evenly distributed over the i age-groups that are specifically affected by such a risk. So, in 2050 for instance, the 32,695 malaria-induced additional deaths are evenly distributed over the 14 different age groups, whereas the 32,955 diarrhoeal-induced additional deaths are evenly distributed over the first three age groups of the population. Third, a given mortality risk increases with climate change without taking into account adaptation, which means that our modeling choice cannot comply with the non-monotonicity over time that the WHO (2014) study estimates for deaths caused by undernutrition, malaria, and diarrhoeal diseases (see Table 5). Fourth, the global temperature increase (or anomaly) is used as a proxy for climate change. This is a crude assumption, as mortality is more likely to depend on more specific climate data such as precipitation or moisture. However, this assumption logically follows the equivalent modeling choice made in both the WHO (2014) study and in most IAMs. Finally, Pottier et al. (2018) have chosen a power-dependency for temperature, akin to the usual damage functions used in climate change economics literature. This power-dependency, θ, the probability of dying with respect to temperature, is the same for each risk, meaning that it does not depend on a given risk j. The sensitivity of the results to this parameter will be tested. Due to space constraints, the calibration procedure of parameters $\alpha_{i,j}$ is detailed in Appendix B.

4.2.2 Simulations

Given the uncertainty surrounding the WHO (2014) study, the simulations presented in this section should only be used to assess the sensitivity, not the outputs, of the excess mortality function due to climate change presented in Eq. 6. We simulated our model with the exogenous GWP of either the *SSP2* or the *Collapse* scenario, together with three different temperature trajectories displayed in Figure 15. The names of the temperature scenarios (*+4°C*, *+3°C*, and *+2°C*) correspond to the temperature anomaly reached in 2100 compared to the pre-industrial era. Given the wide variability of the simulation results of climate models for the same greenhouse gas emission trajectory (i.e, representative concentration pathway, RCP, in the IPCC's lexicon), we did not use the outputs of a

given climate model and chose instead to determine the temperature trajectories in Figure 15 so that they reflect some representative patterns of the IPCC's RCP.

As expected, for a given exogenous GWP trajectory, the higher the temperature increase due to climate change, the lower the population. By calibration (see Appendix B), the number of additional deaths is quite similar across scenarios, and prior to 2050 the number of additional deaths remains below 500,000 per five-year period in each temperature scenario. However, in 2100, the $+4^\circ$ scenario implies about twice as many deaths per five-year period (2.5 millions) than in the $+2^\circ C$ scenario (1.25 millions) when $\theta = 1$, and logically around four times more (4 million compared to less than 1 million) when $\theta = 2$ (Figure 16). If the exogenous GWP of the *Collapse* scenario is used instead of *SSP2*, climate change logically generates a higher number of additional deaths as the total population–in particular the younger cohorts–is larger (Figure 17). For example, in the $+2^\circ C$ scenario when $\theta = 2$, there are approximately 6 million additional deaths per year in 2100 in the *Collapse* scenario, compared to approximately 4 million in the *SSP2* scenario. In order to further test the sensitivity of the excess mortality function associated with climate change, we perform in Appendix C the previous simulations again, replacing the WHO's (2014) estimate of 84,697 nutrition-related additional deaths per year in 2050 with the far higher Springmann et al. (2016) value of 381,000 additional deaths.

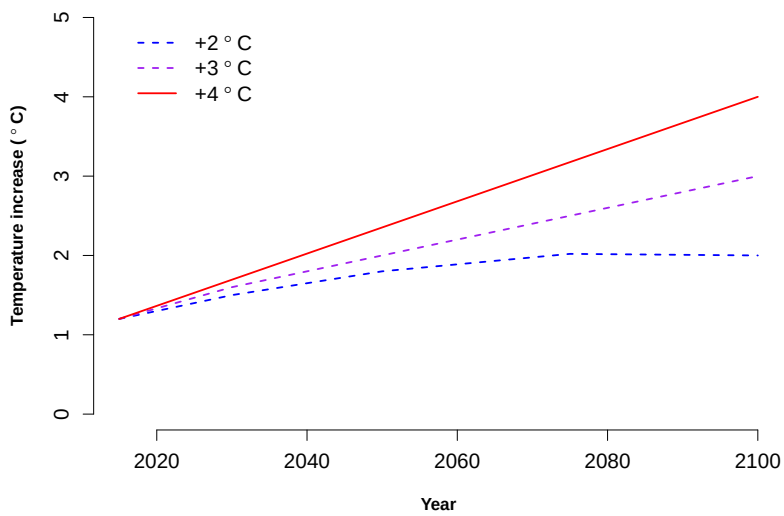

Figure 15: Three scenarios of temperature change from pre-industrial era.

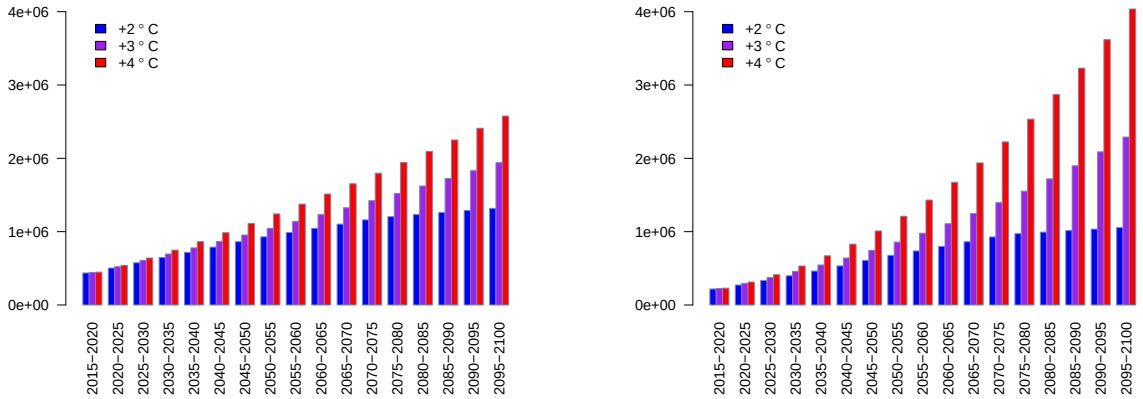

(a) $\theta = 1$ **(b)** $\theta = 2$

Figure 16: Climate change induced deaths every five years with exogenous *SSP2* GWP.

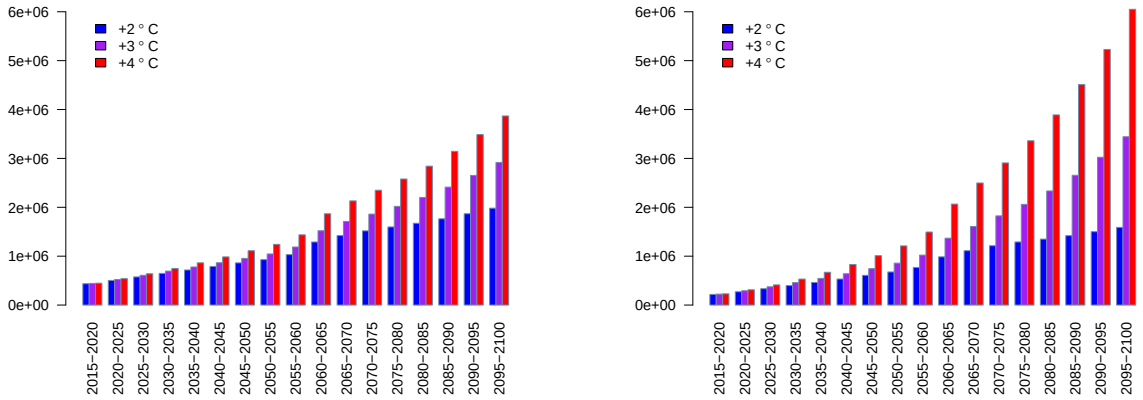

(a) $\theta = 1$ **(b)** $\theta = 2$

Figure 17: Climate change induced deaths every five years with exogenous *Collapse* GWP.

5 Conclusion

Understanding demographic dynamics is undeniably complex, as multiple interconnected factors affect both birth rates and death rates. In this article, we attempted to circumvent this complexity by providing a simple endogenous model of the world human population, with just enough complexity to present an age structure. Using the gross world product as the only exogenous input variable to determine the birth rate and age-specific death rates, we designed a phenomenological model of the global population dynamics.

The analysis of this theoretical model suggested that it is most likely asymptotically unstable, preventing its use in determining the carrying capacity of the Earth. Nevertheless, we showed that our model accurately reproduces the global population dynamics over the period 1950–2015. Moreover, for any prospective scenario of increasing GWP, the model presented in this paper yields consistent outputs. A major implication of this simulation result is that both the United Nations and the IPCC take no account of the historical relationship that prevailed between GWP and population from 1950 to 2015, and thus assume future decoupling possibilities between economic development and fertility that have never been witnessed during the last sixty-five years. On the contrary, in the

case of an abrupt collapse of the economic production, the population dynamics of our model responds with higher deaths rates that are more than compensated for by increasing birth rates. Hence, in such a scenario of collapsing GWP, the population gets relatively larger and younger (i.e., there is an increase in the size of the 0–4 year-old group relative to other age groups). As we noted, this result might appear counter-intuitive at first, in particular if one has in mind the simulation outputs of the *World3* model of Meadows et al. (1972). Yet, we recalled that results in *World3* are driven by negative feedback from the lack of non-renewable resources and unsustainable pollution levels, which combined cause food production to degrowth drastically.

Hence, we then discussed the implementation of environmental negative feedback in our model. In order to comply with existing Integrated Assessment Models, we investigated the sensitivity of our model to an excess mortality function associated with climate change. The calibration of the health-related damage function was performed using the most recent and consistent data from the WHO (2014). Even though it can only yield relative and not absolute outcomes, estimates of additional deaths in 2100 due to climate change range from 1 million per five-year period in a *+2°* scenario to 6 million per five-year period in a *+4°* scenario. These additional deaths caused by climate change hardly affect the world population level reached at the end of 2100. This result could receive two very different interpretations: (i) the estimates of the WHO (2014) study are extremely conservative, or (ii) the results of Meadows et al. (1972) are highly unrealistic because they would imply that the WHO's (2014) estimates should be multiplied by a factor of 100 to 1000.

We acknowledge that the climate change component of the model developed in the present paper is not robust. Nevertheless, this article is, to the best of our knowledge, the first to present a complete endogenous framework of world population dynamics that can both take into account the effects of climate change, and be used into any kind of IAM. We hope that future studies assessing the impact of climate change on additional deaths will be used to better calibrate our model and therefore improve its estimates of the impacts of climate change on human population dynamics.

Appendices

Appendix A: Model sensitivity to changes in the death rate of the fragile population

To test the sensitivity of the model without climate change, we modify the death rate of the fragile population, defined as the first and the last groups (i.e., N_1 and N_{14}), *ceteris paribus* in 2100 (i.e., keeping the GWP from the SSP2 scenario and the birth rate constant). The results are displayed on the heatmap of Figure 18. For instance, this figure indicates that in order to observe a global population of about 4.5 billion people in 2100, as found in the standard run of the (in)famous study of Meadows et al. (1972), the death rate of group N_1 (0–4 years old) would have to be multiplied by about fifteen.

Appendix B: Calibration of excess mortality function associated with climate change

To calibrate the $\alpha_{i,j}$, we borrow the methodology of Pottier et al. (2018). We note that calibrating the $\beta_i := \sum_{j \in J} \alpha_{i,j}$ is sufficient to have the correct assessment of $\widetilde{DR}_i$ without identifying each elements of the set J for a given age-group. We start by simulating the model without climate feedback under *SSP2* scenario, and compute the number of deaths between 2045-2050 for each group. Then, assuming that the increase in temperature T within this period equals T^0 (i.e., the temperature change of +2.5°C in 2050 for the A1b used in the WHO (2014) study), we add the number of death induced by climate change in 2050 that are reported in p. 12 of the WHO (2014)

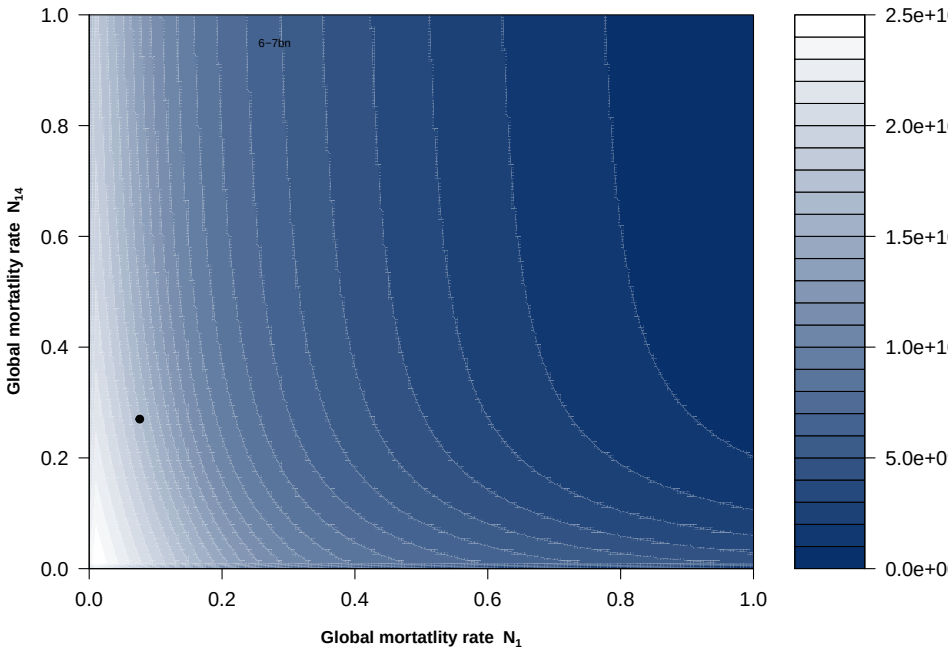

Figure 18: Sensitivity of global population level in 2100 as a function of groups N_1 (0–4 years old) and N_{14} (+65 years old) specific death rates D_1 and D_{14}. The black dot represents the population of about 12 billion attained in the *SSP2 GWP* scenario.

study. As the number of deaths induced by climate change is not evenly distributed over the age-groups, we assume the distribution provided by the WHO (2014) study and reproduced in Table 6. Finally, Table 7 provides the fitted values for parameters β_i.

Table 6: Proportion of the additional deaths provided by WHO (2014) assigned to each age-group

	Undernutrition	Malaria	Dengue	Diarrhoeal diseases	Heat waves
0-4	1	1/14	1/14	1/3	0
5-9	0	1/14	1/14	1/3	0
10-14	0	1/14	1/14	1/3	0
15-19	0	1/14	1/14	0	0
⋮	⋮	⋮	⋮	⋮	⋮
60-64	0	1/14	1/14	0	0
>65	0	1/14	1/14	0	1

Appendix C: Sensitivity analysis of the excess mortality function associated with climate change

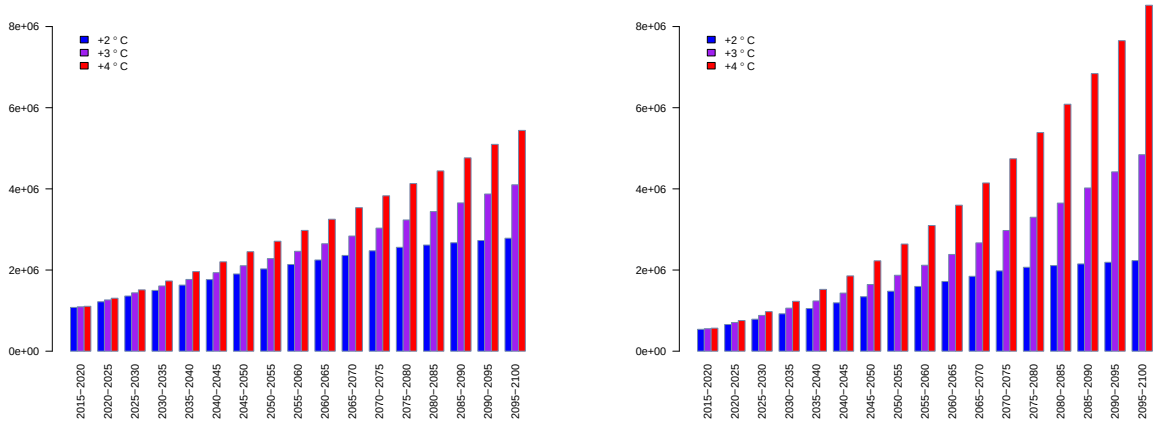

(a) $\theta = 1$ **(b)** $\theta = 2$

Figure 19: Climate change induced deaths every five years with exogenous *SSP2* GWP scenario and Springmann et al.'s (2016) estimates for nutrition-related climate-induced deaths.

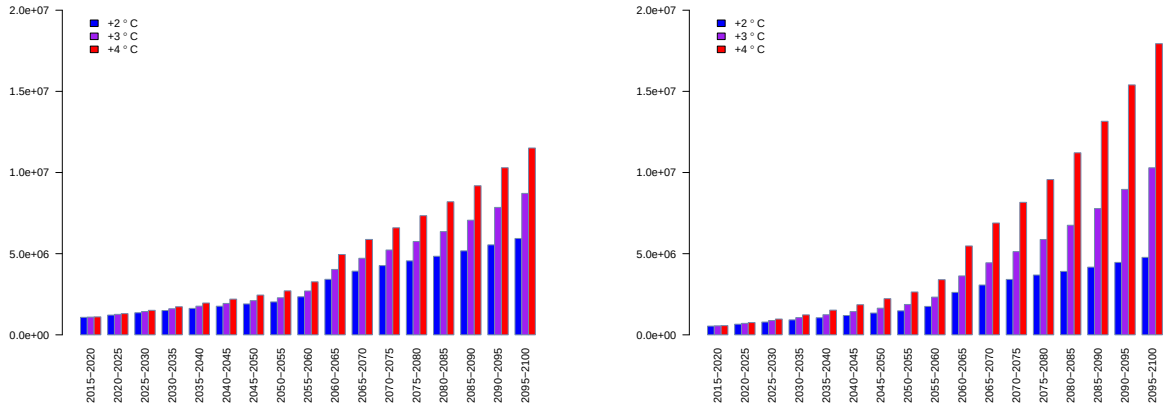

(a) $\theta = 1$ **(b)** $\theta = 2$

Figure 20: Climate change induced deaths every five years with exogenous *Collapse* GWP and Springmann et al.'s (2016) estimates for nutrition-related climate-induced deaths.

Table 7: Calibrated parameter value for all β_i (scale 10^{-2})

β_1	β_2	β_3	β_4	β_5	β_6	β_7
1.607	1.995	2.207	0.291	0.205	0.181	0.159

β_8	β_9	β_{10}	β_{11}	β_{12}	β_{13}	β_{14}
0.142	0.118	0.092	0.066	0.049	0.035	0.143

Table 8: Calibrated parameter value for all β_i (scale 10^{-2}) using Springmann et al.'s (2016) estimates for nutrition-related climate-induced deaths

β_1	β_2	β_3	β_4	β_5	β_6	β_7
6.46	1.995	2.200	0.292	0.205	0.184	0.159

β_8	β_9	β_{10}	β_{11}	β_{12}	β_{13}	β_{14}
0.142	0.118	0.092	0.066	0.048	0.034	0.144

Acknowledgments

This work benefited from the support of the Chair Energy & Prosperity. We thank Emmanuel Bovari and Antoine Godin for their helpful comments on an earlier version of this article. All remaining errors are our own.

References

Akaev, A. A. and Sadovnichii, V. A. (2010). Mathematical model of population dynamics with the world population size stabilizing about a stationary level. *Doklady Mathematics*, 82(3):978–981.

Aral, M. M. (2014). Climate Change and Human Population Dynamics. *Water Quality, Exposure and Health*, 6(1-2):53–62.

Becker, G. S. (1960). An Economic Analysis of Fertility. In Becker, G. S., editor, *Demographic and Economic Change in Developed Countries*. Princeton University Press, Princeton, NJ.

Becker, S. O., Cinnirella, F., and Woessmann, L. (2010). The trade-off between fertility and education: evidence from before the demographic transition. *Journal of Economic Growth*, 15:177–204.

Bolt, J., Inklaar, R., de Jong, H., and van Zanden, J. L. (2013). *Maddison Project Database 2013*. https://www.rug.nl/ggdc/historicaldevelopment/maddison/releases/maddison-project-database-2013.

Cai, D. (2012). An economic growth model with endogenous carrying capacity and demographic transition. *Mathematical and Computer Modelling*, 55(3-4):432–441.

Carlson, E. and Tsvetarsky, S. (2000). Birthweight and infant mortality in Bulgaria's transition crisis. *Paediatric and perinatal epidemiology*, 14(2):159–162.

Carmichael, S., de Pleijt, A., van Zanden, J. L., and De Moor, T. (2016). The European Marriage Pattern and Its Measurement. *Journal of Economic History*, 76(1):196–204.

Chertow, M. R. (2000). The IPAT Equation and Its Variants. *Journal of Industrial Ecology*, 4(4):13–29.

Cohen, J. E. (1995). Population Growth and Earth's Human Carrying Capacity. *Science*, 269:341–346.

Cole, A. and Flenley, J. (2008). Modelling human population change on Easter Island far-from-equilibrium. *Quaternary International*, 184(1):150–165.

Cummins, N. (2013). Marital fertility and wealth during the fertility transition: rural France, 1750-1850. *Economic History Review*, 66(2):449–476.

De Onis, M. (2000). Measuring nutritional status in relation to mortality. *Bulletin of the World Health Organization*, 78(10):1271–1274.

Di, Q., Wang, Y., Zanobetti, A., Wang, Y., Koutrakis, P., Choirat, C., Dominici, F., and Schwartz, J. (2017). Air pollution and mortality in the Medicare population. *New England Journal of Medicine*, 376(26):2513–2522.

Diaz, M. and Moore, f. (2018). Quantifying the economic risks of climate change. *Nature Climate Change*, 7(11):774–782.

Diebolt, C. and Perrin, F. (2013). From stagnation to sustained growth: the role of female empowerment. *American Economic Review*, 103(3):545–549.

Dolgonosov, B. M. (2016). Knowledge production and world population dynamics. *Technological Forecasting and Social Change*, 103:127–141.

Eberlein, R. L. and Thompson, J. P. (2013). Precise modeling of aging populations. *System Dynamics Review*, 29(2):87–101.

Ehrlich, P. R. (1968). *The Population Bomb*. Ballantine Books, New York, NY.

Franchini, M. and Mannucci, P. (2015). Impact on human health of climate changes. *European Journal of Internal Medicine*, 26(1):1—5.

Galor, O. and Mountford, A. (2008). Trading Population for Productivity: Theory and Evidence. *Review of Economic Studies*, 75(4):1143–1179.

Gasparrini, A. et al. (2017). Projections of temperature-related excess mortality under climate change scenarios. *The Lancet Planetary Health*, 1(9):e360–e367.

Goldewijk, K. K., Beusen, A., Doelman, J., and Stehfest, E. (2017). Anthropogenic land use estimates for the Holocene – HYDE 3.2. *Earth System Science Data*, 9:927–953.

Greenwood, J. and Seshadri, A. (2002). The U.S. Demographic Transition. *American Economic Review*, 92(2):153–159.

Guerrini, L. (2013). Analysis of an Economic Growth Model with Variable Carrying Capacity. *International Journal of Mathematical Analysis*, 7(26):1263–1270.

Guha-Sapir, D. and van Panhuis, W. (2003). The importance of conflict-related mortality in civilian populations. *Lancet*, 361(9375):2126–2128.

IPCC (2000). *Special Report on Emissions Scenarios. A Special Report of Working Group III of the Intergovernmental Panel on Climate Change*. Cambridge University Press, Cambridge, UK.

IPCC (2013). *Climate Change 2013: The Physical Science Basis. Contribution of Working Group I to the Fifth Assessment Report of the Intergovernmental Panel on Climate Change*. Cambridge University Press, Cambridge, UK.

IPCC (2014). *Climate Change 2014: Mitigation of Climate Change. Contribution of Working Group III to the Fifth Assessment Report of the Intergovernmental Panel on Climate Change*. Cambridge University Press, Cambridge, UK.

Jerven, M. (2012). An unlevel playing field: national income estimates and reciprocal comparison in global economic history. *Journal of Global History*, 7(1):107–128.

Kolstad, E. and Johansson, K. (2011). Uncertainties associated with quantifying climate change impacts on human health: a case study for diarrhea. *Environmental health perspectives*, 119(3):299–305.

Kremer, M. (1993). Population Growth and Technological Change: One Million B.C. to 1990. *Quarterly Journal of Economics*, 108(3):681–716.

Lee, R. (2003). The Demographic Transition: Three Centuries of Fundamental Change. *Journal of Economic Perspective*, 17(4):167–190.

Luby, S. (2017). Clean water, clean hands or new vaccines? *Journal of Infection*, 74:S18–S22.

Malthus, T. R. (1798). *An Essay on the Principle of Population, as it Affects the Future Improvement of Society with Remarks on the Speculations of Mr. Godwin, M. Condorcet, and Other Writers*. J. Johnson, London, UK.

Meadows, D. H., Meadows, D. L., Randers, J., and Behrens, W. (1972). *The Limits to Growth: A Report for the Club of Rome's Project on the Predicament of Mankind*. Universe Books, New York, NY.

Micó, J. C., Caselles, A., Soler, D., Sanz, M. T., and Martínez, E. (2008). A Side-by-Side Single Sex Age-Structured Human Population Dynamic Model: Exact Solution and Model Validation. *Journal of Mathematical Sociology*, 32(4):285–321.

Micó, J. C., Soler, D., and Caselles, A. (2006). Age-Structured Human Population Dynamics. *Journal of Mathematical Sociology*, 30(1):1–31.

Mora, C., Dousset, B., Caldwell, I., Powell, F., Geronimo, R., Bielecki, C., Counsell, C., Dietrich, B., Johnston, E., Louis, L., Lucas, M., McKenzie, M., Shea, A., Tseng, H., Giambelluca, T., Leon, L., Hawkins, E., and Trauernicht, C. (2017). Global risk of deadly heat. *Nature Climate Change*, 7:501–506.

Murphy, T. (2015). Old habits die hard (sometimes): Can *département* heterogeneity tell us something about the French fertility decline? *Journal of Economic Growth*, 20(2):177–222.

Navarro, A., Moreno, R., Jiménez-Alcázar, A., and Tapiador, F. J. (2017). Coupling population dynamics with earth system models: the POPEM model. *Environmental Science and Pollution Research*, pages 1–12.

Okuducu, M. B. and Aral, M. M. (2017). Knowledge based dynamic human population models. *Technological Forecasting and Social Change*, 122:1–11.

Peri-Rotem, N. (2016). Religion and Fertility in Western Europe: Trends Across Cohorts in Britain, France and the Netherlands. *European Journal of Population*, 32(2):231–265.

Pottier, A., Fleurbaey, M., Méjean, A., and Zuber, S. (2018). Integrated assessment of climate and population change: A first pass. *Working Paper*, pages 1–24.

Prados de la Escosura, L. (2016). Mismeasuring long-run growth: the bias from splicing national accounts—the case of Spain. *Cliometrica*, 10(3):251–275.

Ripple, W. J., Wolf, C., Newsome, T. M., Galetti, M., Alamgir, M., Crist, E., Mahmoud, M. I., and Laurance, W. F. (2017). World Scientists' Warning to Humanity: A Second Notice. *BioScience*, 67(12):1026–1028.

Sanz, M. T., Micó, J. C., Caselles, A., and Soler, D. (2014). A Stochastic Model for Population and Well-Being Dynamics. *Journal of Mathematical Sociology*, 38(2):75–94.

Shkolnikov, V., McKee, M., and Leon, D. (2001). Changes in life expectancy in Russia in the mid-1990s. *Lancet*, 357(9260):917–921.

Smil, V. (2017). *Energy and Civilization: A History*. MIT Press, Cambridge, MA.

Smith, M. and Myers, S. (2018). Impact of anthropogenic CO2 emissions on global human nutrition. *Nature Climate Change*, 8(9):834–839.

Sobotka, T., Skirbekk, V., and Philipov, D. (2011). Economic Recession and Fertility in the Developed World. *Population and Development Review*, 37(2):267–306.

Springmann, M., Mason-D'Croz, D., Robinson, S., Garnett, T., Godfray, H., Charles, J., Gollin, D., Rayner, M., Ballon, P., and Scarborough, P. (2016). Global and regional health effects of future food production under climate change: a modelling study. *The Lancet*, 387(10031):1937–1946.

Tapia Granados, J. and Diez Roux, A. (2009). Life and death during the Great Depression. *Proceedings of the National Academy of Sciences of the United States of America*, 106(41):17290–17295.

Tapia Granados, J. and Ionides, E. (2017). Population health and the economy: Mortality and the Great Recession in Europe. *Health Economics*, 26(12):e219–e235.

Tol, R. S. J. (2018). The Economic Impacts of Climate Change. *Review of Environmental Economics and Policy*, 12(1):4–25.

United Nations (2017a). World Population Prospects: The 2017 Revision, Methodology of the United Nations Population Estimates and Projections. *Department of Economic and Social Affairs, Population Division*.

United Nations (2017b). World Population Prospects: The 2017 Revision, Volume I: Comprehensive Tables. *Department of Economic and Social Affairs, Population Division*.

von Foerster, H., Mora, P. M., and Amiot, L. W. (1960). Doomsday: Friday, 13 November, A.D. 2026. At this date human population will approach infinity if it grows as it has grown in the last two millenia. *Science*, 132(3436):1291–1295.

WHO (2014). *Quantitative risk assessment of the effects of climate change on selected causes of death, 2030s and 2050s*. World Health Organization, Geneva, CH.

World Bank, T. (2018). World Bank Indicators, gross domestic product, constant 2010 US$. https://data.worldbank.org/indicator/NY.GDP.MKTP.KD. Accessed online 11-April-2018.

Wrigley, E. A. (2016). *The Path to Sustained Growth: England's Transition from an Organic Economy to an Industrial Revolution*. Cambridge University Press, Cambridge, UK.